IEEE Access
Multidisciplinary ⋮ Rapid Review ⋮ Open Access Journal

Received 1 August 2023, accepted 10 August 2023, date of publication 14 August 2023, date of current version 18 August 2023.

Digital Object Identifier 10.1109/ACCESS.2023.3305261

RESEARCH ARTICLE

An Auxiliary Classifier Generative Adversarial Network Based Fault Diagnosis for Analog Circuit

YONGQIANG ZHENG AND DONGQING WANG
College of Electrical Engineering, Qingdao University, Qingdao 266071,China
Corresponding author: Dongqing Wang (dqwang64@qdu.edu.cn)

This work was supported by the National Natural Science Foundation of China under Grants 62273190.

ABSTRACT To solve the analog fault diagnosis problem with fewer samples, a transformer based auxiliary classifier generative adversarial network (ACGAN) is investigated for circuit fault diagnosis by constructing both generator and discriminator in ACGAN with pure transformer components. The transformer has high model generality due to its weak inductive bias, but it also increases the risk of overfitting on small datasets. Therefore, we use ACGAN to generate sample data to enrich the dataset and mitigate the overfitting. However, ACGAN is severely unstable during the training period, for this reason, a confidence mechanism for the discriminator is added to improve the classification accuracy and a new layer normalization method for the generator is studied to avoid the loss of conditional information. Take the sallen-key filter circuit and the biquad high-pass filter circuit as the experiment objects. The experiment results indicate that the transformer based ACGAN diagnosis method can effectively improve diagnosis accuracy, reach 96.22% and 95.35%, respectively.

INDEX TERMS Transformer; analog circuit, neural networks, fault diagnosis, auxiliary classifier generative adversarial network (ACGAN).

I. INTRODUCTION

In modern society, electronic equipment is widely used in communications, military, network, consumer electronics and medical industries. According to statistics, more than 60% of electronic products are made with mixed analog/digital integrated circuits. Currently, analog circuits account for only 20% of hybrid circuits [1], [2], [3], [4], [5], [6]. However, due to the complex fault state in analog circuits, the continuity of response signals, the tolerance effect of fault components, and the relatively mature development of fault diagnosis in digital circuits, 80% circuit faults occur in analog circuits [4], [7], [8]. The fault diagnosis of analog devices plays a vital role in the stable operation of systems. Due to the nonlinearity and tolerance of the circuit, the advancement of analog circuit fault diagnosis methods is slow, and unable to play a businesslike role in circuit maintenance. For this reason, scholars over world have carried out a lot of research in this area.

The associate editor coordinating the review of this manuscript and approving it for publication was Guillermo Valencia-Palomo.

A. CLASSIFICATION OF FAULT DIAGNOSIS METHODS

In recent years, regarding the fault diagnosis methods of analog circuit, they can be mainly categorized into analytical model-based methods, knowledge-based (qualitative empirical knowledge) methods and data-driven techniques [9].

i. Model-based approaches require to process accurate quantitative mathematical models, which are robust but tolerant of faults [10]; Concerning model-based methods, Atoui and Cohen proposed a method of Bayesian classifier that combines statistical decision making and fault feature matrices to diagnose both single faults and a mixture of multiple faults [11]. Geetha and Jerome proposed a model-based approach for diagnosing the degree of application of artificial intelligence for dynamic nonlinear CSTR processes, emphasizing the use of fuzzy logic for residual generation and residual evaluation [12].

ii. knowledge-based approaches perform fault diagnosis of analog circuits through intelligent concepts and processing methods [13]. Concerning knowledge-based methods, Beaulah et al. developed a system-based expert solution to diagnose and detect faults [14]. The inference part aims to check the consistency of the input signals and faults; Nan et al. proposed a knowledge-based fault diagnosis method that utilizes the valuable knowledge of experts and operators, as well as real-time data from various sensors,and reasoning is based on fuzzy logic [15].

However, model-based approaches and knowledge-based approaches are more suitable for systems with fewer inputs, outputs, or state variables, and are too costly to use for systems with large amounts of data [16].

iii. Data-driven techniques do not rely on expert experience and do not need to know the exact analytical model, but only need to face an object data, thus greatly simplify the fault detection workflow [9]. The data-driven based fault diagnosis methods include machine learning and black-box data-driven methods.

Research on conventional machine learning based fault diagnosis is mature. For example, Yongkui et al. extracted the fault features from the frequency domain response of the circuit, and used an SVM method for fault classification [17]. Guo et al. used principal component analysis (PCA) as a tool to extract fault features, and applied a wavelet support vector machine (WSVM) to diagnose analog circuit faults [18]. Zhang et al. proposed a combined fault diagnosis method of wavelet packet feature extraction, singular value decomposition (SVD) and dimensionality reduction support vector machine (SVM), which improves the fault diagnosis rate of analog circuits, effectively reduces the amount of matrix computation and accelerates the diagnosis speed [19].

B. DEEP LEARNING BASED FAULT DIAGNOSIS METHODS

Neural network based deep learning are applied in various research and industry fields, such as emotion recognition [20], brain source imaging analysis [21], text classification [21], battery states estimation [22], [23], etc. Now it starts to be used in the field of circuit fault diagnosis [24], [25]. Du et al. studied a convolutional neural network (CNN) based circuit fault diagnosis method, which simplifies the fault diagnosis process and improves the fault diagnosis rate [26]. Zhao et al. explored a deep belief network (DBN) based fault diagnosis method for analog circuits, which adaptively extracts features from the original time series signal and automatically classifies fault modes [27]. Gong and Du proposed an attentional mechanism and convolutional neural network (CBAM-CNN) approach for fault diagnosis in analog circuits [28]. Yang et al. proposed an end-to-end denoising auto-encoder (EEDAE) based fault diagnosis method which includes denoising autoencoder (DAE) and softmax classifier [29].

C. THE MAIN CONTRIBUTIONS

Although the above methods have been widely used in analog circuit troubleshooting, they all have certain limitations. To solve the problems of insufficient training samples and low fault diagnosis accuracy in analog circuit fault diagnosis, this paper proposes a transformer based auxiliary classifier generative adversarial network (ACGAN) for analog circuit fault diagnosis to solve these problems.

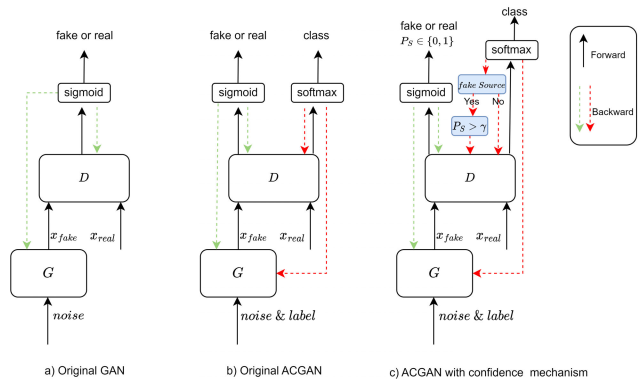

FIGURE 1. **Comparison between ordinary ACGAN and ACGAN with confidence mechanisms.**

Transformer is a new type of neural network with its self-attention mechanism to extract features [30], which can effectively obtain global information, and its multiplicity can be mapped to multiple spaces to enhance the expressive ability of the model. Due to the weak inductive bias, it has a strong generalization ability, but it also increases the risk of overfitting on small datasets. Therefore, we use ACGAN to generate sample data to enrich the dataset and mitigate the overfitting.

The main contributions of this paper are as follows:

(1) For an analog circuit fault diagnosis, a transformer based auxiliary classifier generative adversarial network (ACGAN) is studied by constructing both the generator and the discriminator with transformer units;
(2) Transformer units in ACGAN utilizes the self-attention mechanism to obtain global information, so as to promote diagnosis accuracy and enhance the model's expression power.
(3) A layer normalization regularization method is investigated for the generator, which introduces noises and labels into the computation of the LayerNorm;
(4) A confidence mechanism is added to the discriminator loss function, and the discrimination accuracy of the ACGAN discriminator is greatly improved;
(5) A sallen-key circuit and the biquad high-pass filter circuit are used to verify the validity of the transformer based ACGAN method.

II. THE ACGAN BASED FAULT DIAGNOSIS

A. THE AUXILIARY CLASSIFIER GENERATIVE ADVERSARIAL NETWORK (ACGAN)

Shown in Fig. 1(a), the generative adversarial network (GAN) consists of two important parts: a generator (abbreviated as G) and a discriminator (abbreviated as D) [31], G strives to generate as real samples as possible to make D indistinguishable true and fake, while D tries to distinguish between true and fake data. G and D form a dynamic adversarial, with the progress of training (confrontation), the data generated by G

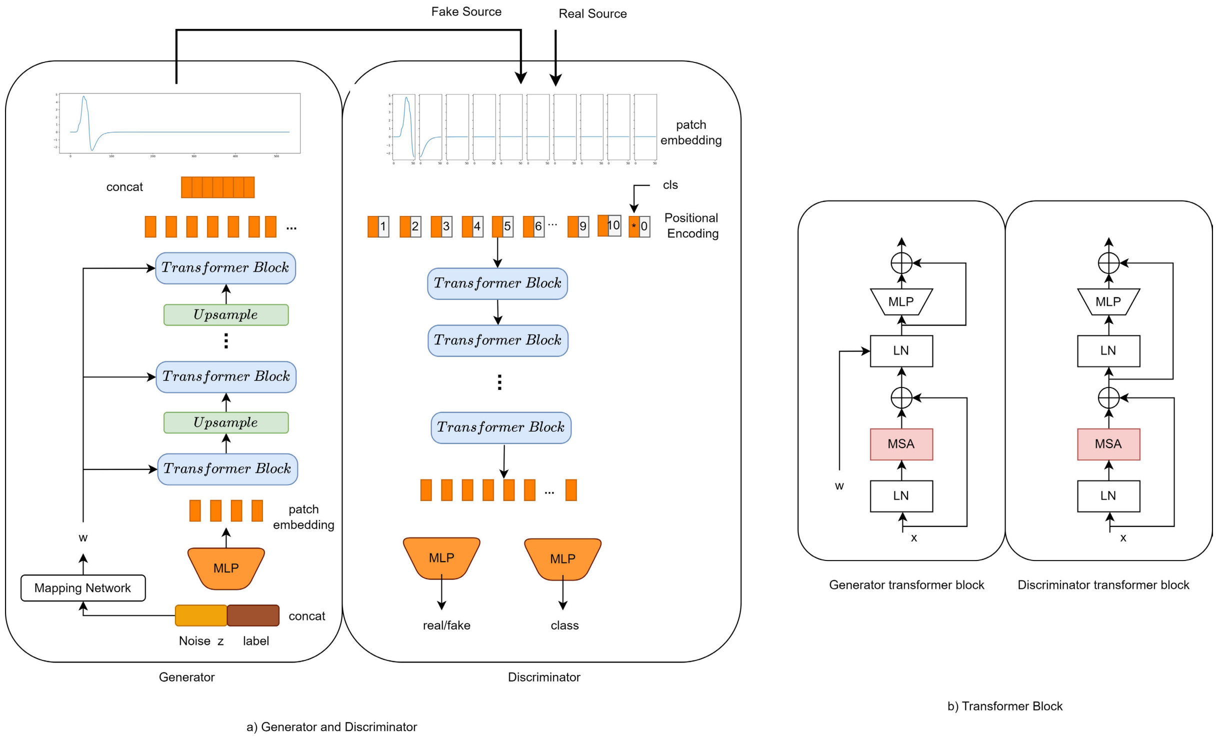

FIGURE 2. **Overall structure.**

is getting closer to the real data, and the level of D discriminating the data is getting higher. Since the original GAN cannot control the category of generated data, conditional generative adversarial network (CGAN) uses category labels as auxiliary information of G to achieve control over the category of generated data [32]. ACGAN further extends the function of D on the basis of CGAN to achieve true-fake discrimination and category differentiation (auxiliary classifier) [33]. Its structure is shown in Fig. 1(b).

(1) The generator G outputs the corresponding category data $X_{fake} = G(noise, label)$ according to the given category label and the noise signal;
(2) The discriminator D gives the probability distribution of the input data (real and fake) and the probability distribution on the class label;
(3) A confidence mechanism is added to the original ACGAN, as shown in Fig. 1(c).

B. TRANSFORMER

Transformers break the limitations of recurrent neural networks (RNN) models, which cannot be computed in parallel, by stacking multiple layers of self-attention and feed-forward neural network layers to extract deeper features. The multiple heads map it to multiple spaces and enhance the model's expression power. The key components of transformer include self-attention, multi-head attention mechanism, and layer normalization. Both the discriminator and generator are constructed using transformers, which allow end-to-end training to extract features without feature engineering. The details are described in the following.

(1) Self-Attention
The self-attention mechanism in transformers allows the model to dynamically weight each position based on information from other positions in the sequence when processing sequence data. It is able to capture the dependencies between different positions in the sequence, and effectively model long-range dependencies. It can be expressed as

$$head_h(X) = softmax(\frac{QK^T}{\sqrt{d_h}})V \tag{1}$$

where X$\in$ $R^{n\times d_X}$ is input, n denotes the length of the input sequence; $Q = XW_Q$, $K = XW_K$, $V = XW_V$; W_Q, W_K, W_V $\in$ $R^{d_X\times d_{model}}$ denotes the projection matrix; d_h denotes the dimension of the h-th attention head.

(2) MultiHead-Attention
The transformer model contains multiple parallel attention heads, each of which learns different attention weights. It can be expressed as

$$MultiHead(X) = concat(head_1, \ldots head_h)W_O \tag{2}$$

where $head_h$ $\in$ $R^{n\times d_{model}}$ denotes the output of the h-th attention header; $W_O \in R^{hd_{model}\times d_{model}}$ denotes the linear transformation matrix.

(3) Layer normalization

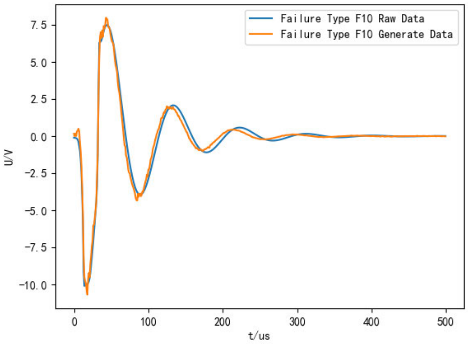

(a) F10 data

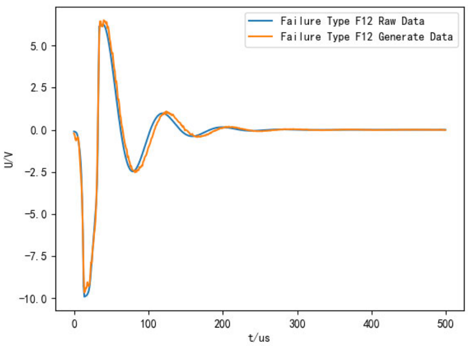

(b) F12 data

FIGURE 3. Comparison of generated and real samples.

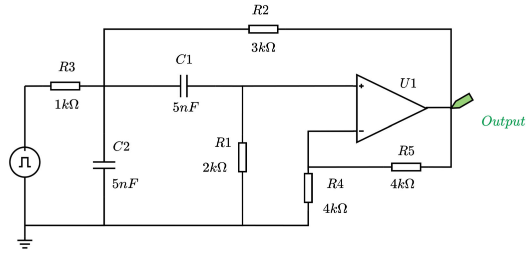

(a) The sallen-key filter circuit

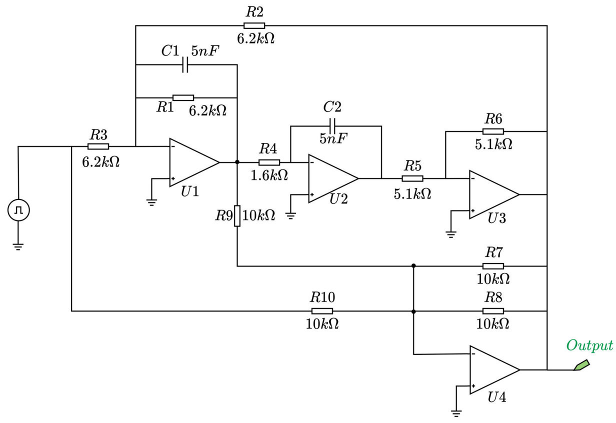

(b) The biquad high-pass filter circuit

FIGURE 4. The experiment circuits.

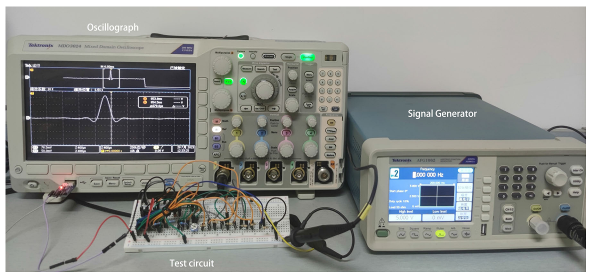

FIGURE 5. Laboratory bench.

The effect of batch normalization is related to the batch size, and the dataset of the fault diagnosis simulation is a small dataset, the effect of batch normalization is not good, so we use layer normalization which is commonly used in transformer. The LayerNorm formula can be written as:

$$\mathrm{LayerNorm}(x) = \frac{x - \mathrm{E}[x]}{\sqrt{\mathrm{var}[x] + \epsilon}} * \gamma + \beta \tag{3}$$

where x is the input, $\mathrm{E}[x]$ is the mean of the input, $\mathrm{var}[x]$ is the variance of the input tensor, ϵ is a very small constant used to prevent dividing by zero, and γ and β are learnable tensors used to control the mean and variance of the input tensor.

C. THE DISCRIMINATOR D

The network architecture of discriminator is shown in Fig. 2(a), which consists of transformer unit, positional encodinng, patch embedding, multilayer perceptron (MLP), and two outputs. The transformer block is shown in Fig. 2(b), and each transformer block in the discriminator consists of MSA, residual shortcut, MLP, and layer normalization. The biggest difference between this transformer neural network and the common neural network is that there are two outputs:

- The first output 'O_1' is used to determine the source of the sample, and the activation function uses the Sigmoid function:

$$f(x_j) = \frac{1}{1 + e^{-x_j}} \tag{4}$$

- The second output 'O_2' is used for classification and the activation function uses the SoftMax activation function:

$$f(x_j) = \frac{e^{-x_j}}{\sum_{c=1} e^{-x_c}} \tag{5}$$

D. THE GENERATOR G

The framework of the generator is shown in Fig. 2(a), the generator mainly consists of transformer blocks, upsampling layer, and MLP. The transformer blocks in the generator is shown in Fig. 2(b). Noise and label are not only used as inputs, but also used to modulate the layer normalization, and their action are:

$$w = Mapping\ network(concat(noise, label)) \tag{6}$$

TABLE 1. The fault types of the TC1.

Early fault codes	Early fault category	Normal	Early fault value
F0	N	-	-
F1	R1↑	$2k\Omega$	2.5kΩ
F2	R1↓	$2k\Omega$	1.5kΩ
F3	R2↑	$3k\Omega$	3.75kΩ
F4	R2↓	$3k\Omega$	2.25kΩ
F5	C1↑	5nF	6.25nF
F6	C1↓	5nF	3.75nF
F7	C2↑	5nF	6.25nF
F8	C2↓	5nF	3.75nF

TABLE 2. The fault types of the TC2.

Early fault codes	Early fault category	Normal	Early fault value
F0	N	-	-
F1	R1↑	$6.2k\Omega$	7.75kΩ
F2	R1↓	$6.2k\Omega$	4.65kΩ
F3	R2↑	$6.2k\Omega$	7.75Ω
F4	R2↓	$6.2k\Omega$	4.65kkΩ
F5	R3↑	$6.2k\Omega$	7.75kΩ
F6	R3↓	$6.2k\Omega$	4.65kkΩ
F7	R4↑	$1.6k\Omega$	2kΩ
F8	R4↓	$1.6k\Omega$	1.2kΩ
F9	C1↑	5nF	6.25nF
F10	C1↓	5nF	3.75nF
F11	C2↑	5nF	6.25nF
F12	C2↓	5nF	3.75nF

TABLE 3. Comparison of different models for TC1.

Methods	Accuracy	F1-Scores	Paramete Num
CBAM-CNN [29]	90.18	90.40	731081
FFT-CNN-LSTM [43]	93.20	93.57	2380809
Proposed method ($\gamma = 0.6$)	96.22	96.45	1609674

TABLE 4. Comparison of different models for TC2.

Methods	Accuracy	F1-Scores	Parameter Num
CBAM-CNN [29]	81.78	80.10	731597
FFT-CNN-LSTM [43]	82.52	82.05	2381837
Proposed method ($\gamma = 0.2$)	95.35	93.97	1610378

TABLE 5. Comparison of different classifiers on TC1.

Method	Average Accuracy	Average F1-Score
ACGAN($\gamma = 0.6$)	96.22	96.45
Discriminator (without Generator)	93.20	93.49

The LayerNorm formula can be rewritten as:

$$\text{LayerNorm}(x) = \frac{x - \text{E}[x]}{\sqrt{\text{var}[x] + \epsilon}} * \gamma(w) + \beta(w) \tag{7}$$

The generator network can generate specific types of sample data by inputting Gaussian white noise and labels to the discriminator for identification to enhance the discriminator's ability to extract features and improve the discriminator's classification ability. Fig. 3 shows that the fake samples generated by the trained generator network are very similar to the real samples in the dataset.

The two classifiers share a feature extraction network, and this paper uses the dummy data generated by G to continuously strengthen the ability of the D-network to extract features, thus greatly improving the classification ability of the discriminator for analog circuit faults, while avoiding the overfitting phenomenon of the network to a certain extent.

TABLE 6. Comparison of different classifiers on TC2.

Method	Average Accuracy	Average F1-Score
ACGAN($\gamma = 0.2$)	95.35	93.44
Discriminator (without Generator)	93.12	93.29

TABLE 7. ACGAN accuracy under different γ on TC1.

Threshold (γ)	Average Accuracy	Average F1-Score
0	95.09	95.36
0.2	95.08	93.45
0.4	95.84	92.79
0.6	96.22	96.45
0.8	95.09	95.33
1.0	95.09	95.37

TABLE 8. ACGAN accuracy under different γ on TC2.

Threshold (γ)	Average Accuracy	Average F1-Score
0	93.68	93.74
0.2	95.35	93.97
0.4	95.16	93.74
0.6	94.60	94.67
0.8	94.05	94.12
1.0	94.42	94.56

E. THE LOSS FUNCTION OF THE ACGAN

Referring to Fig. 1 and its notes, the log-likelihood of the correct source is

$$L_S = E[logP(S = real|X_{real})] + E[logP(S = fake|X_{fake})] \tag{8}$$

The log-likelihood of the correct class of the ordinary ACGAN is

$$L_C = E[\log P(C = c|X_{real})] + E[\log P(C = c|X_{fake})] \tag{9}$$

The loss function of the generator is defined as

$$L_G = L_C - L_S \tag{10}$$

The loss function of the discriminator is defined as

$$L_D = L_C + L_S \tag{11}$$

The rule of the generator and the discriminator is to maximize the L_G and L_D, respectively. The main goal of the ACGAN network is to train the generator that can generate the specified type of data.

In order to train the discriminator with higher classification accuracy, a confidence mechanism is added to the discriminator loss function. The discriminator probability distribution to determine whether the data source is real is

$$P_{FS} = P\left(S = real|X_{fake}\right) \tag{12}$$

The log-likelihood of the correct class with confidence mechanism is defined as

$$\begin{aligned} L_{CC} = E&\left[\log P\left(C = c|X_{real}\right)\right] \\ &+ E\left[\log P\left(C = c|P_{FS} > \gamma\right)\right] \end{aligned} \tag{13}$$

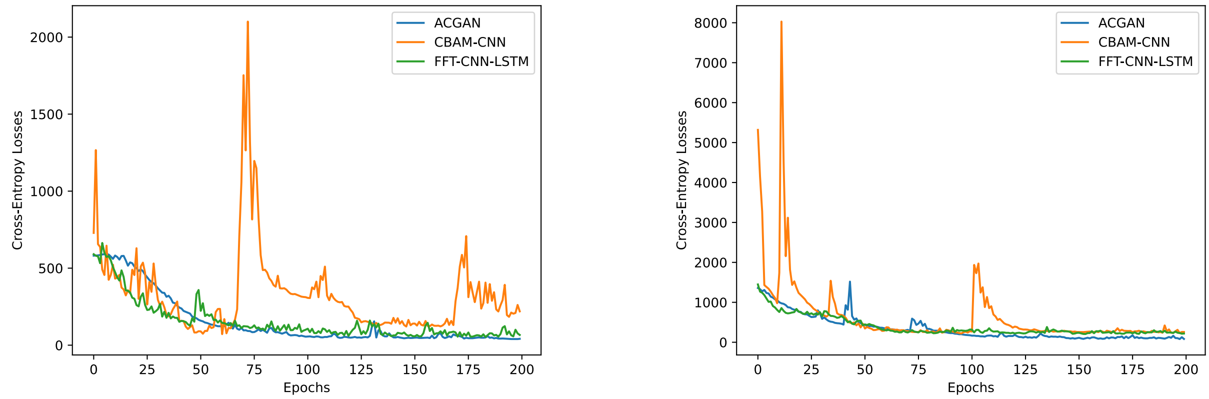

(a) TC1

(b) TC2

FIGURE 6. Loss of different models on TC1 and TC2.

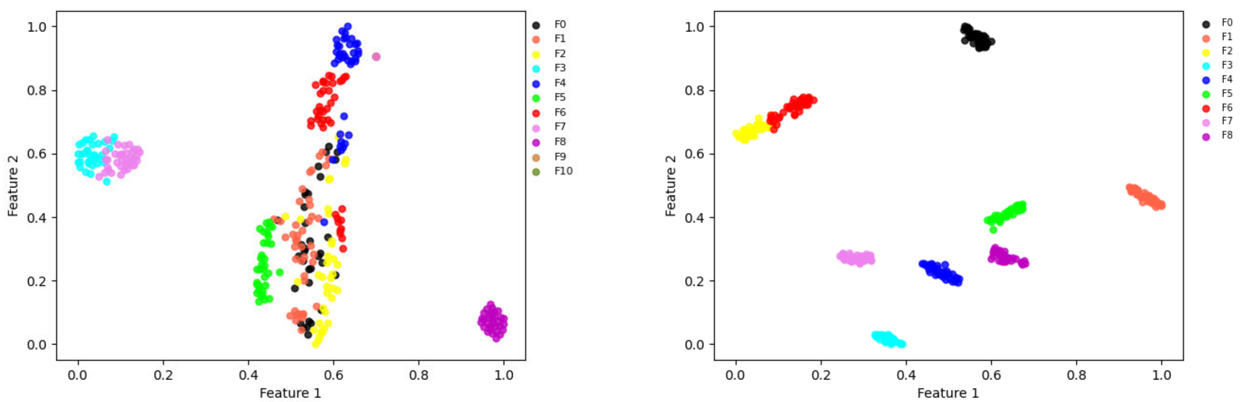

(a) Raw data

(b) Data for feature extraction by ACGAN

FIGURE 7. The spatial distribution of the output data of the TC1.

The discriminator loss function with confidence mechanism as

$$L_D = L_S + L_{CC} \tag{14}$$

When the discriminator determines that the fake data output by the generator is true and the probability of being true exceeds the confidence level, the classification loss function of the false data will affect the discriminator, otherwise it will have no effect on the discriminator.

F. ADAPTIVE MOMENT ESTIMATION (ADAM)

The weight update of G and D networks uses an adaptive moment estimation algorithm, which is widely used for deep learning because of its computational efficiency and ease of use.

Assume t be time step; β_1 and β_2 denote the decay factors of the first and second moment estimation, respectively; $L_M(\theta_M)$ is the objective function ($M \leftarrow G, D$) and its parameter θ_M, its gradient with respect to θ_M at timestep t is

$$g_t = \nabla L_M(\theta_{M,t-1}) \tag{15}$$

Then the first momentum at time step t can be written as

$$m_t = \beta_1 m_{t-1} + (1 - \beta_1) g_t \tag{16}$$

The second momentum at time step t is

$$v_t = \beta_2 v_{t-1} + (1 - \beta_2) g_t^2 \tag{17}$$

The modified first momentum is

$$\hat{m}_t = m_t / (1 - \beta_1^t) \tag{18}$$

The modified second momentum is

$$\hat{v}_t = v_t / (1 - \beta_2^t) \tag{19}$$

The estimated model parameters can be obtained by

$$\theta_{M,t} = \theta_{M,t-1} - \alpha \frac{\hat{m}_t}{\sqrt{\hat{v}_t} + \epsilon} \tag{20}$$

where t represents timestep; $L(\theta_t)$ represents objection function with parameters θ; β_1 and β_2 denote the decay factors of the first and second moment estimation, respectively.

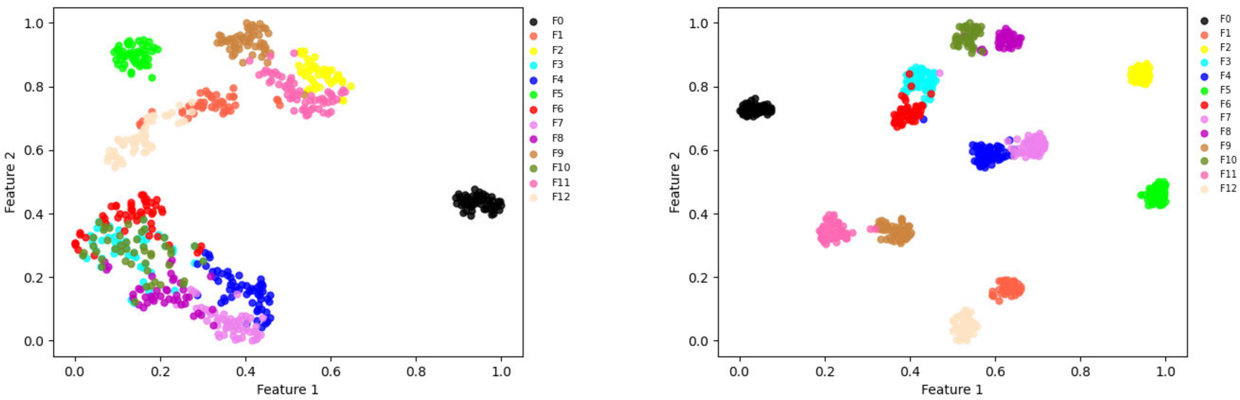

(a) Raw data

(b) Data for feature extraction by ACGAN

FIGURE 8. The spatial distribution of output data of the TC2.

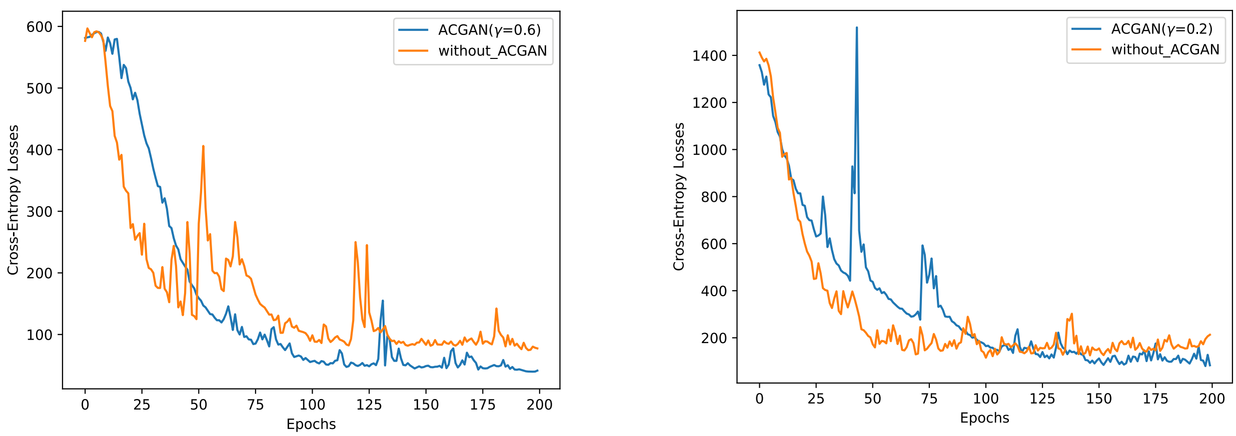

(a) TC1

(b) TC2

FIGURE 9. Loss of different models on TC1 and TC2.

III. EXPERIMENT

A. THE EXPERIMENT OBJECTS

In the experiments of this paper, the sallen-key filter circuit (TC1) [34], [35], [36], [37] and the biquad high-pass filter ciruit (TC2) [34], [35], [36], [37] are taken as the objects, as shown in Fig. 4. The actual circuit experiment bench is set up, as shown in the Fig. 5. The conditions are as follows.

- The excitation source input adopts a pulse wave with a duratio of 10us and an amplitude of $10V$, and the fault time domain response signal is sampled at the output point.
- The tolerance range of the resistor in the circuit is set to 5% [38], and the tolerance [39] range of the capacitor is set to 10%.
- When the parameter value of a component in a circuit departs from the normal value by 25%, the component can be considered to have an early fault. The types of faults for the two circuits under test are shown in Tables 1 and 2.
- 40 Monte Carlo (Gaussian distribution) simulations were implemented for each fault class, and the sample length collected for each simulation analysis is 500 points.
- The dataset is split using the hold-out method, with 60% dataset as a training set and 40% dataset as a test set.

B. COMPARATIVE EXPERIMENT

1) CIRCUIT FAULT DIAGNOSIS WITH DIFFERENT MODELS

Taking TC1 and TC2 circuits as experiment subjects, under different number of datasets, compare fault diagnosis accuracy of the proposed transformer based ACGAN method with the other two methods as follows.

(1) In [40], [41] mentioned two methods, the number of samples per fault type is 100; while in the proposed method, that is 40.

(2) Tables 3-4 show that the proposed method achieves 96.22% and 95.35% respectively on the two test circuits, which are better than the other two methods.

(3) From the training validation loss in Fig. 6, it can also be seen that the training effect of the proposed transformer based ACGAN is better than the other two methods.

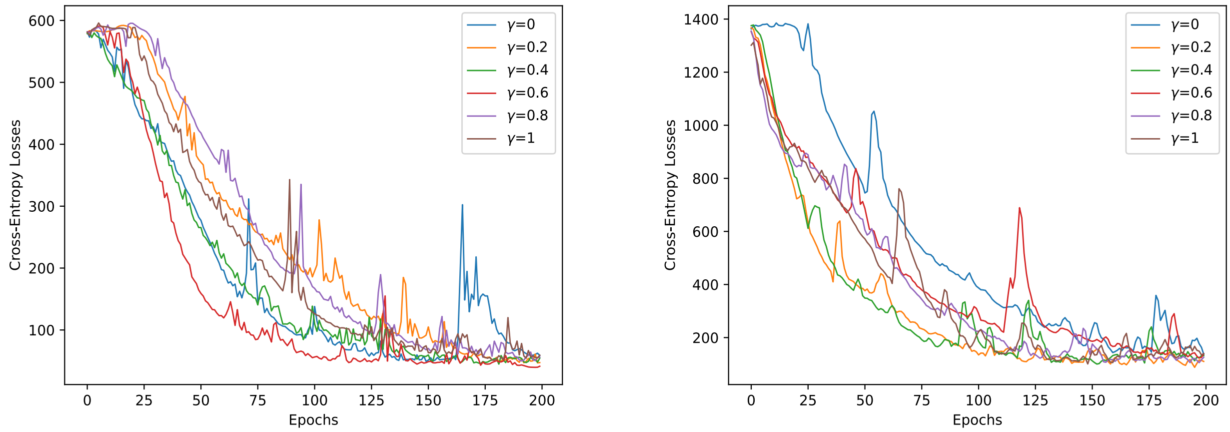

(a) TC1

(b) TC2

FIGURE 10. **Loss of different confidence levels on TC1 and TC2.**

(4) The proposed transformer based ACGAN gets better performance on small dataset.

2) FEATURE EXTRACTION

To demonstrate the feature extraction capability of the proposed method, Figs. 7 and 8 visualize the original data and the features extracted by the ACGAN. T-distributed stochastic neighbor embedding (T-SNE) dimensionality reduction on the collected circuit output features, extracted two principal components and visualized them, as shown in Figs. 7(a) and 8(a). The data of various types of faults have obvious overlap, which is not conducive to the fault classification.

T-SNE reduces the features extracted by Discriminator in Fig. 2(a) to 2 dimensions, and draw its spatial distribution as shown in Figs. 7(b) and 8(b). It can be clearly seen that after the features being extracted by the Discriminator, all kinds of fault feature data are distributed independently, with good aggregation and far distribution.

C. THE ABLATION TEST

1) FAULT DIAGNOSIS WITH/WITHOUT THE ACGAN ARCHITECTURE

To further validate the effectiveness of our designed ACGAN architecture constructed from pure transformer units (with a discriminator and a generator), We compared it with a general classifier constructed from transformer units, which only has the discriminator (without the generator) on ablation experiments using the TC1 and TC2 as objects. The experiments are conducted under threshold $\gamma = 0.2$ and $\gamma = 0.6$, the results are shown in Tables 5-6, and the training validation loss function is shown in Fig. 9. We have the follow conclusions

- Training with general classifier (only with Discriminator), the average accuracy of the classifier for five tests is only 93.20% and 93.12% on test circuits TC1 and TC2;
- Training with ACGAN model (Discriminator and Generator), the average accuracy of the classifier for five tests reach 96.22% and 95.35%, an improvement of 3.02% and 2.23%, respectively.
- The results indicate that ACGAN effectively improves the classification accuracy of the discriminator with limited samples.

2) CIRCUIT FAULT DIAGNOSIS WITH DIFFERENT CONFIDENCE LEVELS

In this part, the classification accuracy influence of the threshold (γ) in formula (6) is studied. Under 6 thresholds γ=0, 0.2, 0.4, 0.6, 0.8 and 1.0, we take 5 simulations on each threshold and take the average value as results. The experiment results are shown in Tables 7-8, the training validation loss function is shown in Fig. 10.

The result analysis is as follows:

- When the $\gamma = 0$, it is an ACGAN network without confidence mechanism, the fault diagnosis accuracy of the ACGAN network classifier are 95.09% and 93.68%, which is even inferior to the general transformer model. The reason is the bad influence of generated data with low confidence level on the discriminator classifier training.
- When the threshold value $\gamma = 0.2$, the accuracy reaches 95.35% on test circuit TC2, which is 1.67% improvement than $\gamma = 0$. This show that different γ has a great impact on the accuracy.
- When the threshold value $\gamma = 0.6$, the accuracy reaches 96.22% on test circuit TC1, which is 1.13% than $\gamma = 0$.
- When the $\gamma = 1$, the fault diagnosis accuracy of the ACGAN network classifier are 95.09% and 94.42%. At this time, the network system is the same as CGAN.

IV. CONCLUSION

For nonlinear analog circuits, a confidence mechanism aided transformer based ACGAN network is investigated to diagnose their faults with high diagnosis accuracy. Take the sallen-key filter circuit and the biquad high-pass filter circuit as the experiment objects. The results show that the modified ACGAN based diagnosis method can effectively improve the diagnosis accuracy, reaching 96.22% and 95.35%, respectively. From the experiments, the following conclusions are obtained.

- The discriminator built by pure transformers has strong feature extraction capability.
- The improved LayerNorm can effectively avoid the loss of conditional information, so that the generator can produce data with specific labels.
- The ACGAN system constructed by pure transformers avoids model overfitting caused by too few samples, and the fake samples produced by the generator enhances the classification ability of the classifier to a certain extent, and the accuracy is improved by 3.02% and 2.23%, respectively.
- The confidence mechanism included in the correct loss function for classification avoids the detrimental effect of low confidence in the generated data on classification. By choosing an appropriate threshold, the accuracy can be improved to some extent, such as by 1.13% on TC1 and 1.67% on TC2 over the model without the confidence mechanism.

DECLARATION OF INTERESTS

The authors declare that they have no known competing financial interests or personal relationships that could have appeared to influence the work reported in this paper.

DATA AVAILABILITY STATEMENT

The data related to this work are available from the corresponding author upon reasonable request.

REFERENCES

[1] G. Fedi, S. Manetti, and M. Piccirilli, "Comments on, 'linear circuit fault diagnosis using neuromorphic analyzers,'" *IEEE Trans. Circuits Syst. II, Analog Digital Signal Process.*, vol. 46, no. 4, pp. 483–485, Apr. 1999.

[2] M. Aminian and F. Aminian, "Neural-network based analog-circuit fault diagnosis using wavelet transform as preprocessor," *IEEE Trans. Circuits Syst. II, Analog Digit. Signal Process.*, vol. 47, no. 2, pp. 151–156, Feb. 2000.

[3] Y. Cui, J. Shi, and Z. Wang, "Analog circuits fault diagnosis using multi-valued Fisher's fuzzy decision tree (MFFDT)," *Int. J. Circuit Theory Appl.*, vol. 44, no. 1, pp. 240–260, Jan. 2016.

[4] Y.-H. Chang, "Frequency-domain grouping robust fault diagnosis for analog circuits with uncertainties," *Int. J. Circuit Theory Appl.*, vol. 30, no. 1, pp. 65–86, 2002.

[5] H. Feng, G. Li, J. Yu, X. Ma, and J. Wang, "Analog circuit fault diagnosis based on enhanced Harris Hawks optimization algorithm with RBF neutral network," *Eng. Rep.*, vol. 5, no. 6, Jun. 2023, Art. no. e12634.

[6] A. Arabi, M. Ayad, N. Bourouba, M. Benziane, I. Griche, S. S. M. Ghoneim, E. Ali, M. Elsisi, and R. N. R. Ghaly, "An efficient method for faults diagnosis in analog circuits based on machine learning classifiers," *Alexandria Eng. J.*, vol. 77, pp. 109–125, Aug. 2023.

[7] M. Worsman and M. W. T. Wong, "Non-linear analog circuit fault diagnosis with large change sensitivity," *Int. J. Circuit Theory Appl.*, vol. 28, no. 3, pp. 281–303, May 2000.

[8] H. Sira-Ramírez, A. Hernández-Méndez, J. Linares-Flores, and A. Luviano-Juárez, "Robust flat filtering DSP based control of the boost converter," *Control Theory Technol.*, vol. 14, no. 3, pp. 224–236, Aug. 2016.

[9] C. Zhang, S. Zhao, Z. Yang, and Y. He, "A multi-fault diagnosis method for lithium-ion battery pack using curvilinear Manhattan distance evaluation and voltage difference analysis," *J. Energy Storage*, vol. 67, Sep. 2023, Art. no. 107575.

[10] A. Biasizzo and F. Novak, "A methodology for model-based diagnosis of analogue circuits," *Appl. Artif. Intell.*, vol. 14, no. 3, pp. 253–269, Mar. 2000.

[11] M. A. Atoui and A. Cohen, "Coupling data-driven and model-based methods to improve fault diagnosis," *Comput. Ind.*, vol. 128, Jun. 2021, Art. no. 103401.

[12] M. Geetha and J. Jerome, "Fuzzy expert system based sensor and actuator fault diagnosis for continuous stirred tank reactor," in *Proc. Int. Conf. Fuzzy Theory Appl. (iFUZZY)*, 2013, pp. 251–257.

[13] S. Xu, "A survey of knowledge-based intelligent fault diagnosis techniques," *J. Phys., Conf. Ser.*, vol. 1187, no. 3, Apr. 2019, Art. no. 032006.

[14] S. A. Beaulah, Z. S. Chalabi, and D. G. Randle, "A real-time knowledge-based system for intelligent monitoring in complex, sensor-rich environments," *Comput. Electron. Agricult.*, vol. 21, no. 1, pp. 53–68, Sep. 1998.

[15] C. Nan, F. Khan, and M. T. Iqbal, "Real-time fault diagnosis using knowledge-based expert system," *Process Saf. Environ. Protection*, vol. 86, no. 1, pp. 55–71, Jan. 2008.

[16] D. Li, Y. Wang, J. Wang, C. Wang, and Y. Duan, "Recent advances in sensor fault diagnosis: A review," *Sens. Actuators A, Phys.*, vol. 309, Jul. 2020, Art. no. 111990.

[17] S. Yongkui, C. Guangju, and L. Hui, "Analog circuits fault diagnosis based on support vector machine," in *Proc. 8th Int. Conf. Electron. Meas. Instrum.*, Aug. 2007, pp. 3-630–3-634.

[18] K. Guo, S. Wang, and J. Song, "Analog circuit fault diagnosis based on wavelet kernel support vector machine," in *Proc. Int. Conf. Inf. Technol. Appl.*, Chengdu, China, 2013, pp. 395–399.

[19] Y. Zhang, A. Zhang, and D. Yu, "Fault diagnosis of analog circuit based on wavelet packet analysis and SVD," in *Proc. IEEE 19th Int. Conf. Ind. Informat. (INDIN)*, Jul. 2021, pp. 1–6.

[20] Y. Zheng, J. Ding, F. Liu, and D. Wang, "Adaptive neural decision tree for EEG based emotion recognition," *Inf. Sci.*, vol. 643, Sep. 2023, Art. no. 119160.

[21] M. Jiao, G. Wan, Y. Guo, D. Wang, H. Liu, J. Xiang, and F. Liu, "A graph Fourier transform based bidirectional long short-term memory neural network for electrophysiological source imaging," *Frontiers Neurosci.*, vol. 16, Apr. 2022, Art. no. 867466.

[22] M. Jiao and D. Wang, "The Savitzky-Golay filter based bidirectional long short-term memory network for SOC estimation," *Int. J. Energy Res.*, vol. 45, no. 13, pp. 19467–19480, Oct. 2021.

[23] T. Gu, D. Wang, and Y. Li, "A Polak-Ribière-Polyak conjugate gradient algorithm optimized broad learning system for lithium-ion battery state of health estimation," *J. Electrochem. Soc.*, vol. 169, no. 9, Sep. 2022, Art. no. 090512.

[24] S. Tang, S. Yuan, and Y. Zhu, "Data preprocessing techniques in convolutional neural network based on fault diagnosis towards rotating machinery," *IEEE Access*, vol. 8, pp. 149487–149496, 2020.

[25] S. Tang, S. Yuan, and Y. Zhu, "Deep learning-based intelligent fault diagnosis methods toward rotating machinery," *IEEE Access*, vol. 8, pp. 9335–9346, 2020.

[26] T. Du, H. Zhang, and L. Wang, "Analogue circuit fault diagnosis based on convolution neural network," *Electron. Lett.*, vol. 55, no. 24, pp. 1277–1279, Nov. 2019.

[27] G. Zhao, X. Liu, B. Zhang, Y. Liu, G. Niu, and C. Hu, "A novel approach for analog circuit fault diagnosis based on deep belief network," *Measurement*, vol. 121, pp. 170–178, Jun. 2018.

[28] B. Gong and X. Du, "Research on analog circuit fault diagnosis based on CBAM-CNN," in *Proc. IEEE Int. Conf. Electron. Technol., Commun. Inf. (ICETCI)*, Aug. 2021, pp. 258–261.

[29] Y. Yang, L. Wang, H. Chen, and C. Wang, "An end-to-end denoising autoencoder-based deep neural network approach for fault diagnosis of analog circuit," *Anal. Integr. Circuits Signal Process.*, vol. 107, no. 3, pp. 605–616, Jun. 2021.

[30] K. Wu, H. Peng, M. Chen, J. Fu, and H. Chao, "Rethinking and improving relative position encoding for vision transformer," in *Proc. IEEE/CVF Int. Conf. Comput. Vis. (ICCV)*, Oct. 2021, pp. 10013–10021.

[31] I. Goodfellow, J. Pouget-Abadie, M. Mirza, B. Xu, D. Warde-Farley, S. Ozair, A. Courville, and Y. Bengio, "Generative adversarial networks," *Commun. ACM*, vol. 63, no. 11, pp. 139–144, 2020.

[32] M. Mirza and S. Osindero, "Conditional generative adversarial nets," 2014, *arXiv:1411.1784*.

[33] A. Odena, C. Olah, and J. Shlens, "Conditional image synthesis with auxiliary classifier GANs," in *Proc. 34th Int. Conf. Mach. Learn.*, 2016, pp. 2642–2651.

[34] J. Cui and Y. Wang, "A novel approach of analog circuit fault diagnosis using support vector machines classifier," *Measurement*, vol. 44, no. 1, pp. 281–289, Jan. 2011.

[35] P. Song, Y. He, and W. Cui, "Statistical property feature extraction based on FRFT for fault diagnosis of analog circuits," *Anal. Integr. Circuits Signal Process.*, vol. 87, no. 3, pp. 427–436, Jun. 2016.

[36] P. Tamilselvan and P. Wang, "Failure diagnosis using deep belief learning based health state classification," *Rel. Eng. Syst. Saf.*, vol. 115, pp. 124–135, Jul. 2013.

[37] P. Chen, L. Yuan, Y. He, and S. Luo, "An improved SVM classifier based on double chains quantum genetic algorithm and its application in analogue circuit diagnosis," *Neurocomputing*, vol. 211, pp. 202–211, Oct. 2016.

[38] L. Dong, A. Mandali, A. Morinec, and Y. Zhao, "Active disturbance rejection based load frequency control and voltage regulation in power systems," *Control Theory Technol.*, vol. 16, no. 4, pp. 336–350, Nov. 2018.

[39] M. Tadeusiewicz, S. Hałgas, and M. Korzybski, "Multiple catastrophic fault diagnosis of analog circuits considering the component tolerances," *Int. J. Circuit Theory Appl.*, vol. 40, no. 10, pp. 1041–1052, Oct. 2012.

[40] Z. Chaolong, H. Yigang, and L. Renxiong, "An analog circuit fault diagnosis approach using DBN as a preprocessor," *Int. J. Circuits, Syst. Signal Process.*, vol. 13, pp. 156–161, Mar. 2019.

[41] C. Zhang, Y. He, T. Yang, B. Zhang, and J. Wu, "An analog circuit fault diagnosis approach based on improved wavelet transform and MKELM," *Circuits, Syst., Signal Process.*, vol. 41, no. 3, pp. 1255–1286, Mar. 2022.

[42] B. Sun, W. Xu, and Q. Yang, "Analog circuit fault diagnosis based on FFT-CNN-LSTM," in *Proc. 7th Annu. Int. Conf. Netw. Inf. Syst. Comput. (ICNISC)*, Jul. 2021, pp. 305–310.

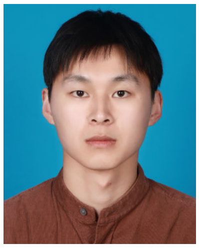

YONGQIANG ZHENG received the B.S. degree from the College of Electrical Engineering, Lanzhou Jiaotong University, Lanzhou, China. He is currently pursuing the Graduate degree with the College of Electrical Engineering, Qingdao University, Qingdao, China. His research interests include nonlinear system identification and deep learning.

DONGQING WANG received the Ph.D. degree in power electronics and power transmission from the College of Automation Engineering, Tianjin University, Tianjin, China, in 2006. She joined the College of Electrical Engineering, Qingdao University, Qingdao, China, in 1988, where she has been a Professor in complex system modeling with the College of Electrical Engineering, since 2011. She was a Visiting Scholar with the Department of Electrical and Computer Engineering, The University of Tennessee, Knoxville, TN, USA, from August 2004 to February 2005. Her research interests include system modeling, machine learning, and EEG signal analysis.